Experimental determination of the solubility of Au in silicate melts

Article *in* Mineralogy and Petrology · September 1996

DOI: 10.1007/BF01162608

CITATIONS
78

READS
76

2 authors:

Alexander Borisov
Russian Academy of Sciences
99 PUBLICATIONS **1,785** CITATIONS
SEE PROFILE

H. Palme
Senckenberg Research Institute
665 PUBLICATIONS **18,182** CITATIONS
SEE PROFILE

Mineralogy and Petrology (1996) 56: 297–312

Mineralogy and Petrology

Experimental determination of the solubility of Au in silicate melts

A. Borisov[1] and **H. Palme**[2]

[1] Vernadsky Institute of Geochemistry and Analytical Chemistry, Russian Academy of Sciences, Moscow, Russia
[2] Mineralogisch-Petrographisches Institut, Universität zu Köln, Köln, Federal Republic of Germany

With 5 Figures

Received March 31, 1995;
accepted September 15, 1995

Summary

We report here new data on the solubility of Au in silicate melts of anorthite-diopside eutectic composition at a wide range of oxygen fugacities, from pure oxygen to 10^{-8} atm, and at a temperature range of 1300 °C to 1480 °C. Because experiments were done with metal loops at temperatures above the Au-melting temperature, PdAu-metal-alloys had to be used. Pd-solubility data derived from the same set of experiments agree with earlier data obtained from experiments with pure Pd-metal (*Borisov* et al., 1994a). The results of the present experiments show that Pd-solubilities are by a factor of 2 to 6 higher than Au-solubilities. Both, Au and Pd solubilities decrease with decreasing oxygen fugacity. At oxygen fugacities below the iron-wüstite buffer (IW) Au solubility increases with decreasing fO_2 probably reflecting formation of Au-silicides at such reducing conditions. Compared to Pd, Au has higher activity coefficients in Fe-metal and lower solubility in silicate melts. This leads to similar metal-silicate partition coefficients for both elements. At a temperature of 1350 °C and an oxygen fugacity corresponding to IW-2 D^{Au} (met/sil) is about $2.5 \cdot 10^7$ and D^{Pd} (met/sil) about $1.6 \cdot 10^7$. Thus similar behavior is expected during metal separation in planetary bodies including core formation in the Earth. The metal/silicate partition coefficient of Ir is, however, by several orders of magnitudes higher (*Borisov* and *Palme*, 1995a). Equilibration with chondritic metal will therefore lead to grossly non-chondritic Pd/Ir or Au/Ir ratios in coexisting silicate phases. Chondritic ratios are thus indicative of the presence of unfractionated meteoritic components. Samples from the upper mantle of the Earth, for example, reflect the admixture of a late unfractionated (chondritic) veneer (e.g., *Kimura* et al., 1974; *Jagoutz* et al., 1979).

Solubilities of Pd and Au in silicate melts are much higher than the contents in terrestrial basalts implying that the abundances of these two elements are not buffered by residual PGE- and Au-containing alloys. The most likely process for fractionating PGEs in terrestrial magmas are mineral-melt (e.g., olivine/melt) equilibria.

Zusammenfassung

Experimentelle Bestimmung der Löslichkeit von Au in Silikatschmelzen

In der vorliegenden Arbeit wird über die Ergebnisse der Bestimmung der Löslichkeit von Au in Silikatschmelzen mit der Zusammensetzung des Anorthit-Diopsid Eutektikums berichtet. Die Versuche wurden mittels Metallschlaufe über einen weiten Sauerstoffpartialdruckbereich, von reinem Sauerstoff bis zu 10^{-8} atm und in einem Temperaturbereich von 1300 °C bis 1480 °C, durchgeführt. Da diese Temperaturen jedoch den Au-Schmelzpunkt überschreiten, wurde mit AuPd-Legierungen gearbeitet. Die Ergebnisse der dadurch zusätzlich erhaltenen Pd-Versuche stimmen mit früher bestimmten, mit reinen Pd-Schlaufen durchgeführten Pd-Löslichkkeiten überein (*Borisov* et al., 1994a). Die auf reine Metalle zurückgerechneten Löslichkeiten von Pd sind um einen Faktor 2 bis 6 mal höher als die entsprechenden Au-Löslichkeiten. Die Löslichkeiten beider Metalle nehmen mit abnehmendem Sauerstoffpartialdruck ab. Unter noch stärker reduzierenden Bedingungen (Eisen-Wüstit Gleichgewicht) nimmt die Löslichkeit von Au jedoch zu. Dies könnte auf die Bildung von Au-Siliziden zurückzuführen sein.

Im Vergleich zu Pd sind die Aktivitätskoeffizienten von Au in metallischem Eisen höher, die Löslichkeiten in Silikatschmelzen jedoch niedriger. Das führt zu ähnlichen Metall/Silikat Verteilungskoeffizienten von Au und Pd. Bei einer Temperatur von 1350 °C und einer Sauerstoffugazität von IW-2 ergeben sich für D^{Au} (met/sil) $2.5 \cdot 10^7$ und für D^{Pd} (met/sil) $1.6*10^7$. Der Metall/Silikat-Verteilungskoeffizient von Ir ist jedoch unter den gleichen Bedingungen um mehrere Größenordnungen höher (*Borisov* and *Palme*, 1995a). Ein chondritisches Pd/Ir- oder Au/Ir-Verhältnis kann also auf die Anwesenheit einer unfraktionierten chondritischen Komponente zurückgeführt werden. Dies gilt beispielsweise für Proben aus dem oberen Erdmantel. Hier handelt es sich vermutlich um Zumischung einer späten chondritischen Akkretionskomponente, die sich nicht mehr mit einer metallischen Phase (Kern) ins Gleichgewicht gesetzt hat (z.B. *Kimura* et al., 1974; *Jagoutz* et al., 1979).

Die Löslichkeiten von Pd und Au in Silikatschmelzen sind wesentlich höher als ihre Gehalte in basaltischen und komatiitischen Laven. Dies bedeutet, daß Au und Pd in Schmelzen aus dem Erdmantel nicht durch residuale Au- und/oder Pd-haltige Metallphasen bestimmt sind. Gleichgewichte zwischen Schmelze und Mineralen (z.B. Olivin) sind die wahrscheinlichsten Fraktionierungsmechanismen für Platingruppenelemente in terrestrischen Magmen.

Introduction

The elements Ir, Os, Ru, Rh, Pt, Pd and Au are called highly siderophile elements (HSE) because they have very high metal/silicate partition coefficients. A small metal fraction is sufficient to extract these elements more or less completely from silicate melts. However, until recently the absolute values of the metal/silicate partition coefficients of HSE were completely unknown. Early determinations for Au gave metal/silicate partition coefficients of around 3.3×10^4 (*Kimura* et al., 1974). *Rammensee* (1978) obtained about $2 \cdot 10^5$ for Ir and $7 \cdot 10^4$ for Au. *Jones* and *Drake* (1986) reported values of $2 \cdot 10^4$ to $2 \cdot 10^5$ for Au and Ir respectively. From this and earlier papers it is clear that realistic metal/silicate partition coefficients are higher by several orders of magnitudes.

A major difficulty in determining these partition coefficients is the low concentrations of HSE in silicates in equilibrium with metallic iron. It is experimentally much

easier to study equilibria between pure metals and silicate melts, i.e., solubilities of the HSE in silicate melts. From solubility data metal/silicate partition coefficients can be extracted if the solution properties of the HSE in metallic iron are known (*Borisov* et al., 1994a). From this type of experimental data three major conclusions have emerged: (1) HSE dissolve as oxides in silicate melts. Metal/silicate partition coefficients are therefore dependent on oxygen fugacity. Partition coefficients increase with decreasing oxygen fugacity (*Borisov* and *Palme*, 1995b). (2) Metal/silicate partition coefficients are higher than previously thought. At an oxygen fugacity two orders of magnitude below the iron-wüstite buffer (IW-2), which is relevant for core formation, the metal/silicate partition coefficient for Pd is about 10^7 (*Borisov* et al., 1994a) while for Ir a value of 10^{12} was found (*Borisov* and *Palme*, 1995a). (3) There are large differences between partition coefficients of HSE as shown above. The important implication is that during metal separation these elements behave differently and a chondritic abundance pattern (relative abundances) is destroyed by metal/silicate partitioning. The behavior of Au is in this context of some interest. Au has a similar vapor pressure as Pd and its behaviour during formation of komatitic lavas and subsequent olivine fractionation is similar to that of Pd (*Brügmann* et al., 1987). *Barnes* et al. (1985) suggested that the major factor determining the fractionation of PGE metals in the Earth is the solubility of PGE in silicate magmas. This may also be true for Au. Further data on the solubilities of these elements may therefore provide new insights into their behavior in terrestrial and extraterrestrial magmatic systems.

Experimental procedures

Preparation of samples

All experiments were conducted in one atm vertical tube furnace with controlled oxygen fugacity (see *Borisov* et al., 1994a, for details). Uncertainties of cited log fO_2 values and temperatures do not exceed ± 0.1 and $\pm 2\,^{\circ}C$, respectively. The experiments were made with a loop technique. Silicates were inserted in metal loops consisting of Au_{45} Pd_{55} and Au_{26} Pd_{74} alloys (at. %). Pure gold-loops could not be used because of the low melting point of Au (1064 °C). Starting materials were commercially available Pd and Au powders (Heraeus, Hanau), which were mixed in appropriate proportions and melted in alumina crucibles at 1550–1600 °C for about 10 minutes in air. The resulting metal balls were hammered to a foil with a thickness of 0.1–0.2 mm. Narrow metal bands, up to 1 mm wide, were cut from the foil and loops with a maximum diameter of 2.5 mm were formed.

Silicates with compositions close to the anorthite-diopside eutectic were produced by mixing diopside and anorthite in the appropriate proportions. The pure minerals were prepared by a gel technique according to procedures described by *Hamilton* and *Henderson* (1968). Silicate powders mixed with a glue were inserted into the loops, and these were then suspended on a ceramic disk and transferred into the furnace. Samples were quenched by quickly withdrawing the ceramic disk from the hot zone to the top of the furnace, and metal-loops and glasses were mechanically separated. Glass samples were polished before analysis to remove possible Au and Pd contamination.

Glasses were analyzed by instrumental neutron activation analysis (INAA) according to the procedure described in *Borisov* et al. (1994a). Since the alloy compositions changed during the experiments, due to evaporative loss of Au, they were determined after the

experiments. Alloys were analyzed with an SEM (Hitachi 450) equipped with a Si-detector for energy dispersive analysis (Kevex-system). The accuracy of the SEM analyses was checked by analyzing the initial alloy composition. The results agreed within 5% of the prepared alloy composition. At least 3 points of each loop were analyzed for Au and Pd, preferably in areas near the contact with the silicate melt. Because of Au evaporation reversed experiments were not possible. In their Pd-experiments *Borisov* et al. (1994a) have done reversed experiments with initially higher than equilibrium contents of Pd in the glasses. The same results were obtained indicating that equilibrium was indeed achieved. In addition *Borisov* et al. (1994a) demonstrated homogeneous distribution of Pd in the glasses by successive removal of the surface layers of the glass and redetermining the Pd contents. Since we have used here the same type of experiment and since we obtained the same results for Pd (see below) we assume that equilibrium was reached and that Au is homogeneously distributed in the silicate glass.

Neutron activation analysis

Silicate glasses were irradiated in the TRIGA-reactor of the Institut für Kernchemie at the Universität Mainz. The neutron flux was $7 \cdot 10^{11}$ n/(cm^2·sec) and duration of irradiation was 6 hours. The 88.1 keV line of ^{109}Pd ($T_{1/2} = 13.8$ h) was used for identification and quantitative analysis of Pd. For Au the 411.8 keV line of ^{198}Au ($T_{1/2} = 2.69$ d) was used. Barium was, as a contaminant of the starting materials, present in all samples at a level of 3200 ppm. The Ba-peak (^{131}Ba, 496 keV) was therefore used as internal standard to monitor INAA procedures (only samples with the correct Ba-content were considered). Countings were performed on small intrinsic Ge detectors to avoid unnecessary compton background produced in high volume Ge-detectors. Pd- and Au-standards were irradiated under the same conditions as the samples. The sensitivity of the method is such that Pd at the 1 ppm level in a sample of 5 mg can be analyzed with a precision of $\pm 10\%$. Repeated analysis of different Pd-standards lead us to believe that accuracy is in the same range as precision. As Au is more sensitive for INAA than Pd the combined error in the Au analysis (precision) is estimated to be less than 3% in all cases.

Thermodynamic data of Au-containing alloys

Before discussing the experimental results we will briefly review the available thermodynamic data on Au-Pd and Au-Fe alloys. Since we want to derive metal-silicate partition coefficients from the experimental results we have to recalculate our results to the solubility of pure Au-metal in silicate melts. This requires the knowledge of activity coefficients of Au in PdAu alloys and in Fe-metal.

(a) Au-Pd solid solution

Thermodynamic data for Au-Pd alloys are published in papers by *Kubaschewski* and *Counsell* (1971) and by *Okamoto* and *Massalsky* (1985). The latter authors concluded that their data are compatible with the Au-Pd phase diagram. Expressions for enthalpy of mixing (ΔH^{mix}, J/mol) and excess entropy of mixing (ΔS^{ex}, J/mol·K) for binary Au-Pd alloys as given by *Okamoto* and *Massalsky* (1985) are:

$$\Delta H^{mix} = X_{Pd} \cdot X_{Au} \cdot (33790 \cdot X_{Pd} - 46614) \quad (1)$$

$$\Delta S^{ex} = -12.552 \cdot X_{Pd} \cdot X_{Au} \quad (2)$$

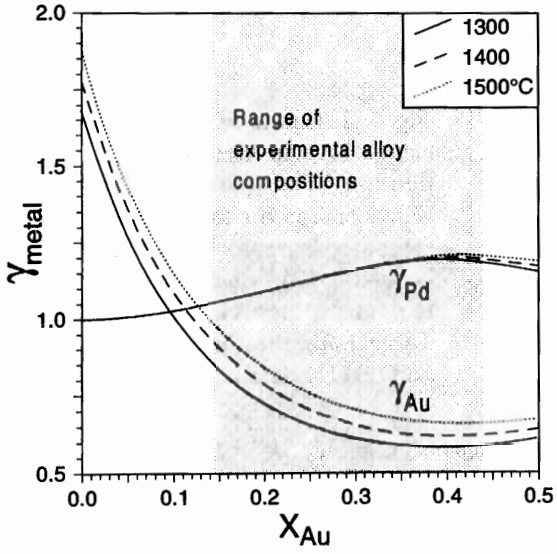

Fig. 1. Activity coefficients for AuPd-alloys derived from thermodynamic data of the AuPd-system (see text for details)

Applying the formalism of asymmetric solid solution (*Thompson*, 1967) leads to:

$$\Delta G^{ex} = X_{Pd} \cdot X_{Au} \cdot (W^G_{PdAu} \cdot X_{Au} + W^G_{AuPd} \cdot X_{Pd}) \quad (3)$$

$$W^G_{ij} = W^H_{ij} - T \cdot W^S_{ij} \quad (i, j = \text{Au, Pd}) \quad (4)$$

where W^G_{AuPd} and W^G_{PdAu} are interaction parameters and X_i are the corresponding mole fractions.

The comparison of (1) and (2) with (3) and (4) yields:

$$W^H_{PdAu} = -46614,\ W^H_{AuPd} = -12824,\ W^S_{AuPd} = W^S_{PdAu} = 12.552$$

The Au and Pd activity coefficients are then calculated from:

$$RT \cdot \ln \gamma_{Au} = (X_{Pd})^2 \cdot [W^G_{PdAu} + 2 \cdot X_{Au} \cdot (W^G_{AuPd} - W^G_{PdAu})] \quad (5)$$

$$RT \cdot \ln \gamma_{Pd} = (X_{Au})^2 \cdot [W^G_{AuPd} + 2 \cdot X_{Pd} \cdot (W^G_{PdAu} - W^G_{AuPd})] \quad (6)$$

Figure 1 shows calculated activity coefficients as a function of the mole fraction of Au in PdAu-alloys, as calculated from equations (5) and (6). These calculations show that the temperature dependencies of γ_{Pd} and γ_{Au} are relatively small for alloy compositions that are relevant for our experiments (X_{Au} from 0.14 to 0.44). Activity coefficients of Pd (γ_{Pd}) are slightly above and activity coefficients of Au (γ_{Au}) somewhat below unity (Fig. 1).

(b) Au-activity in metallic iron at trace levels of Au

The calculation of Au metal/silicate partition coefficients from experimental data of Au-solubilities requires information of γ_{Au} in metallic Fe at $X_{Au} \Rightarrow 0$ (see discussion for Pd in *Borisov* et al., 1994a). Unfortunately, thermodynamic data in the Au-poor part of the Fe-Au system are absent (see *Hultgren* et al., 1973). We therefore chose to estimate these data by comparing the thermodynamic properties of Pd-containing alloys with those of Au-containing alloys.

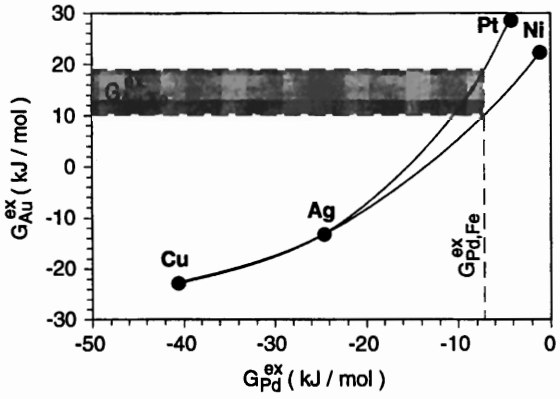

Fig. 2. Estimate of the activity coefficient of Au in metallic Fe at infinite dilution. The partial molar excess Gibbs energy for the Fe-Au system is estimated from the known partial molar excess Gibbs energy of Fe-Pd system and other known systems. See Table 1 for the thermodynamic data and text for details

Table 1. *Partial excess Gibbs energy (J/mol) and partial enthalpy (J/mol*K) values for Au-Me ($X_{Au} = 0$) and Pd-Me ($X_{Pd} = 0$) binarys at 1200 K*

Binary	$(\overline{\Delta G}^{ex})_{Au,i}$	$(\overline{\Delta H})_{Au,i}$	$(\overline{\Delta G}^{ex})_{Pd,i}$	$(\overline{\Delta H})_{Pd,i}$
Ag-Me	−13484.2	−20292.4	−24518.2	–
Cu-Me	−22772.7	−16401.3	−40469.3	−45605.6
Ni-Me	21979.4	27698.1	−945.584	8468.42
Pt-Me	28329.8	23811.1	−4104.54	−12639.9
Fe-Me	–	–	−6839.2	36103.7

For this purpose we have collected the available information in the literature on the partial excess Gibbs energy, $\overline{\Delta G}^{ex}$, for a variety of Au-Me and Pd-Me (Me = Ni, Cu etc.) binary alloys. In Fig. 2 we have plotted the $(\overline{\Delta G}^{ex})_{Au}$ vs. $(\overline{\Delta G}^{ex})_{Pd}$ for four different elements. From the known $(\overline{\Delta G}^{ex})_{Pd,Fe}$ value (Fe-Pd system) a value for $(\overline{\Delta G}^{ex})_{Au,Fe}$ (Fe-Au system) can be estimated. The activity coefficient of Au in metallic Fe is then calculated from:

$$RT \cdot \log \gamma_{Au} = (\overline{\Delta G}^{ex})_{Au,Fe} \tag{7}$$

For 1200 K, $(\overline{\Delta G}^{ex})_{Au,Fe} = 14.5 \pm 4.5$ kJ/mol according to Fig. 2. This is equivalent to $\gamma_{Au} = 4.3 \pm 3$. For comparison $\gamma_{Pd} = 0.504$ at the same temperature. The thermodynamic data used for constructing Fig. 2 and calculating the Au-activity coefficient are summarized in Table 1 (only for $T = 1200$ K). Unfortunately, information on partial excess enthapy $\overline{\Delta H}$, is even more scarce (Table 1) and extrapolations are uncertain. The estimated value of $\overline{\Delta H}_{Au,Fe} = 32$ kJ/(mol·K) is close to $\overline{\Delta H}_{Pd,Fe} = 36.1$ kJ/(mol K), assuming similar temperature dependencies for γ_{Au} and γ_{Pd}.

Results

Experimental results for 26 samples are compiled in Table 2. Besides Pd and Au contents in silicate glasses, alloy compositions, determined by energy dispersive

Table 2. *Experimental results of determination of Au- and Pd-solubilities in silicate melts*

No.	Temp. (C)	Gas mixture	$-\log fO_2$	Duration (hours)	X_{Au} in alloy	Content in glass		Solubilities*	
						Pd, ppm	Au, ppm	Pd, ppm	Au, ppm
1	1302	air	0.68	83	0.440	104.6	7.96	158.6	31.3
2	1301	CO/CO_2	6.54	72	0.415	2.97	0.321	4.30	1.34
3	1303	$CO/CO_2/N_2$	8.30	82	0.403	1.27	0.122	1.80	0.526
4	1302	$CO/CO_2/N_2$	9.13	76	0.397	1.03	0.121	1.45	0.529
5	1300	$CO/CO_2/N_2$	9.97	74	0.409	0.852	0.069	1.22	0.293
6	1300	$CO/CO_2/N_2$	10.51	75	0.394	0.720	0.073	1.00	0.323
7	1301	$CO/CO_2/N_2$	10.99	71	0.402	0.509	0.077	0.719	0.333
8	1303	$CO/CO_2/N_2$	11.46	78	0.352	0.535	0.073	0.703	0.356
9	1403	O_2	0.00	48	0.452	217.5	14.30	335.5	51.2
10	1402	air	0.68	50	0.375	166.9	11.97	225.8	51.6
11	1402	CO_2/N_2	3.34	50	0.336	29.6	2.48	38.1	11.7
12	1403	$CO/CO_2/N_2$	6.03	49	0.412	6.03	0.528	8.63	2.09
13	1398	$CO/CO_2/N_2$	7.47	33–47	0.333	2.89	0.227	3.71	1.08
14	1398	$CO/CO_2/N_2$	8.67	50	0.339	1.80	0.160	2.33	0.751
15	1404	$H_2/CO_2/N_2$	9.10	47	0.160	1.85	0.080	2.08	0.570
16	1404	$H_2/CO_2/N_2$	9.95	45	0.167	1.38	0.081	1.56	0.566
17	1404	$H_2/CO_2/N_2$	9.95	45	0.142	1.61	0.093	1.79	0.704
18	1399	$CO/CO_2/N_2$	10.42	44	0.331	1.05	0.218	1.34	1.04
19	1483	air	0.68	24	0.244	263.8	7.28	313.2	39.7
20	1483	CO_2/N_2	3.07	24	0.161	68.4	1.64	77.0	11.0
21	1481	$CO/CO_2/N_2$	6.51	24	0.182	9.12	0.265	10.4	1.68
22	1481	$CO/CO_2/N_2$	7.37	17–21	0.190	6.49	0.232	7.44	1.44
23	1314	air	0.68	78	0.423	119.5	9.12	175.2	37.1
24	1349	air	0.68	71	0.352	137.7	10.66	180.8	50.3
25	1369	air	0.68	61	0.415	138.7	11.42	200.1	45.7
26	1428	air	0.68	43	0.359	172.3	9.56	228.0	42.1

* Recalculated to solubilities (equilibrium with pure Au- and pure Pd-metal)

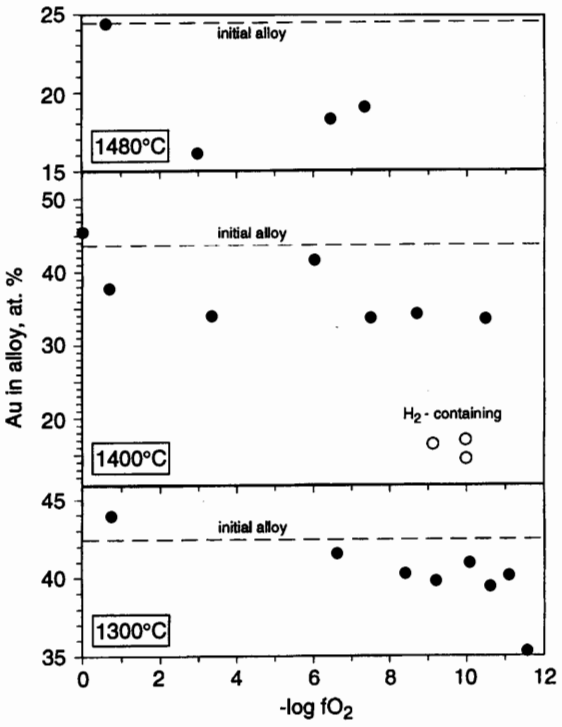

Fig. 3. The Au-contents of the PdAu-alloys determined *after* the experiments at three different temperatures indicating considerable loss of Au at all three temperatures. A trend for higher losses at more reducing conditions is indicated. If H_2-containing gases are used for monitoring fO_2 even higher losses of Au are found. Open symbols: H_2-containing gases; full symbols: H_2-free gases

analysis are also shown. Earlier we have mentioned loss of Au from the alloy during the experiments. The Au-contents of the PdAu-alloys determined after the experiments at three different temperatures are shown in Fig. 3. There is considerable loss of Au at all three temperatures. A trend for higher losses at more reducing conditions is indicated. If H_2-bearing gases are used for imposing fO_2 even higher losses of Au are found (up to 70% of the initial content). The large losses of Au (compared to Pd) can be readily seen from Table 2 and Fig. 3. Because of this, most experiments were conducted with CO-containing gas mixtures. We wish to emphasize that there is not only loss of Au but also loss of Pd from the alloys, in particular during experiments at reducing conditions as can be judged from a strong decrease in thickness of the metal loop band. Changes in alloy composition reflect relatively higher losses of Au compared to Pd.

The measured concentrations of Au and Pd in the silicate glasses were recalculated to solubilities with pure metals by dividing the concentrations by the corresponding activities a_{Me} in the alloy (a_{Me} = mole fraction times activity coefficient). These data are given in the last two columns of Table 2.

Comparison with literature data

To our knowledge the data reported here are the only data for Au-solubilities in silicate melts covering such a wide range of oxygen fugacities. *Capobianco* (1990) reported experimental results for Au-solubility in glasses in equilibrium with solid PdAu alloys. However, he only performed experiments under oxidizing conditions, i.e., in air. The Au-solubility in his experiments is 41 ± 7 ppm at 1450 °C (calculated

from the concentration of Au in the silicate divided by the activity in the metal, c_{Au}/a_{Au}, and assuming $\gamma_{Au} = 1$). This is about 30% higher than our results of 23–30 ppm (at 1430–1480 °C). The difference may reflect compositional differences between the two silicate melt compositions. The silicate melt in Capobianco's experiments contained 10% CaO and 30% Al_2O_3 compared to 25% CaO and 13% Al_2O_3 in the glasses used in the experiments reported here.

Gold solubilities in glassy materials were widely discussed in papers dealing with so called "gold-ruby glasses" (see *Weyl*, 1951, for details). However, the Au-contents of these glasses are much higher than those discussed here and, in addition, these glasses contain large contents of Pb or Sn oxides.

Discussion

Dependence of Au- and Pd-solubility on oxygen fugacity

In Fig. 4 (a–d) the experimental results of Au and Pd-solubilities at three different temperatures are plotted against log fO_2. On the left hand side of Fig. 4 solubilities are calculated assuming ideal solid solution in the PdAu alloy, i.e., concentrations are divided by the mole fractions in the metals (c_{Me}/X_{Me}, $\gamma_{Au} = \gamma_{Pd} = 1$). On the right hand side we have plotted solubilities calculated from concentrations divided by the activities (c_{Me}/a_{Me}, $\gamma_{Au} \neq \gamma_{Pd} \neq 1$). The comparison between the two should allow some estimate of the error introduced by uncertainties of activity coefficients in metals.

We will first discuss Pd-solubilities (Fig. 4a, b). Experiments of *Borisov* et al. (1994a) on Pd solubility in equilibrium with pure Pd, made with the same silicate compositions, allow us to use Pd as a kind of internal standard for the present experiments. As can be seen from Fig. 4a, b there is excellent agreement between the present data and the *Borisov* et al. data. The agreement is best at reducing conditions, where the data points of *Borisov* et al. (1994a) for 1350 °C (stars) are located exactly between the present data points for 1300 °C (filled circles) and 1400 °C (open triangles). The indicated line is redrawn from Fig. 3 in *Borisov* et al. (1994a). In the present experiments the increase in slope at fO_2s above 10^{-3} atm is not so well defined as in the earlier data. At a constant temperature results of all experiments at oxidizing conditions, up to pure oxygen, can be fitted with a single line with a slope close to $\frac{1}{4}$ (Table 3), implying an effective valence of Pd in the silicate melt of around 1+ according to the reaction:

$$Pd(Me) + 1/4 \cdot O_2 = Pd^{1+}O_{1/2} \quad (8)$$

On the other hand, at fO_2s more reducing then 10^{-7} atm, there is definite decrease of the slope to 0.14 ± 0.01 (Table 3), which is close to 0.17 ± 0.01 found by *Borisov* et al. (1994a). This slope implies an effective valence less than 1+ (about $Pd^{0.5+}$), which requires the addition of metallic Pd (Pd^0) either in the form of a single complex with Pd^{2+} or as a mixture of Pd^0 with Pd species of higher valence, dissolved in silicate melt (see *Borisov* et al., 1994a for a detailed discussion). The good agreement of the present experimental results obtained by using PdAu alloys with the earlier results employing pure Pd metal, demonstrates, that in the present experiments equilibrium was reached and that the analyzed silicates are not contaminated with metals but that we are measuring real solubilities.

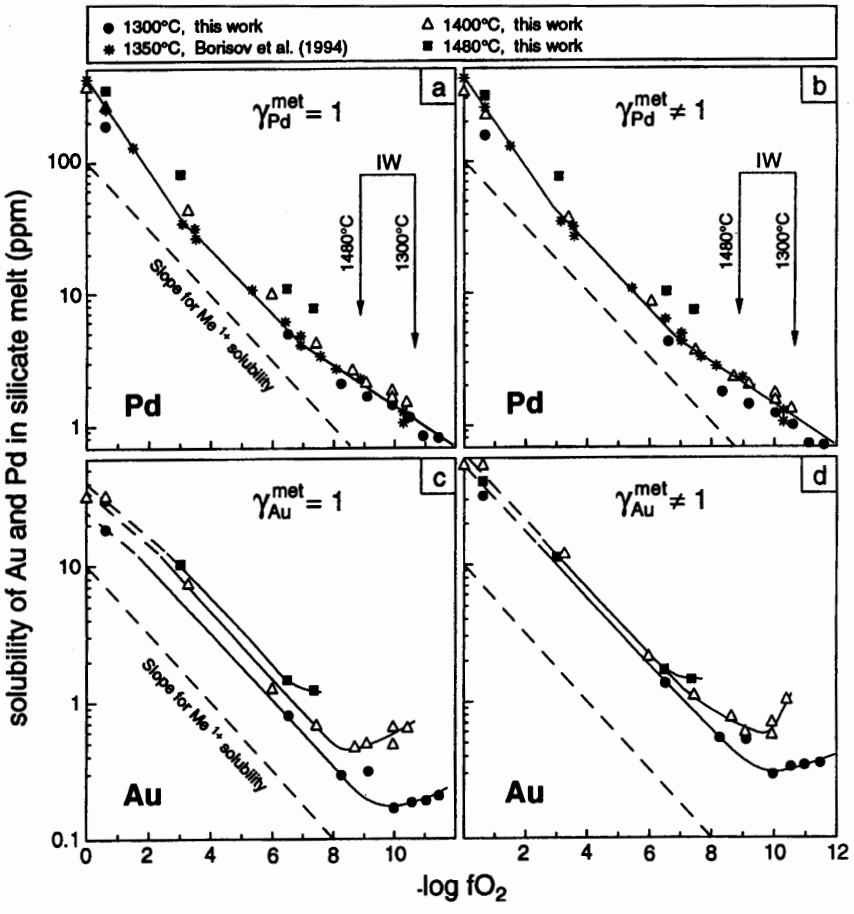

Fig. 4. Experimental results of Au and Pd-solubilities at three different temperatures are plotted against log fO_2. In Fig. 4 a and c solubilities are calculated assuming ideal solid solution in the PdAu alloy, i.e., concentrations are divided by the mole fractions in the metals (c_{Me}/X_{Me}, $\gamma_{Au} = \gamma_{Pd} = 1$). In Fig. 4 b and d solubilities were calculated from concentrations divided by the activities (c_{Me}/a_{Me}, $\gamma_{Au} \neq \gamma_{Pd} \neq 1$). The comparison between the two should allow some estimate of the error introduced by uncertainties of activity coefficients in metals (see text for activity coefficients). Experimental data with pure Pd at 1350 °C are shown for comparison (*Borisov* et al., 1994a)

Gold solubility data are plotted in the lower part of Fig. 4 (c, d). To facilitate the discussion we divide the fO_2 range into three regions which show different behaviour of gold solubility: Region I, with fO_2 from 1 to 10^{-3} atm, region II, from 10^{-3} to 10^{-7}, and region III, below 10^{-7} atm. In region II the slope of gold solubility vs. fO_2 is close to 1/4, implying Au^{1+} as the stable species in silicate melts. This valence for gold is known, although Au_2O_3 is much more stable and a common gold oxide (*Gmelin*, 1992, pp. 59–83). The Au-behavior is analogous to the behavior of Pd found by *Borisov* et al. (1994a) where Pd_2O was found to be the stable oxide species in the melt over a large range of fO_2s although PdO is a much more stable oxide.

In region I a slight decrease of the slope cannot be excluded. This would be unusual because it would imply less oxidized Au at higher fO_2. This trend is,

Table 3. *Slope of log (Pd solubility) vs. log fO_2 and effective valence of Pd in silicate melts*

Conditions (Nos. of experiments)	(Pd/X_{Pd}) slope	(r^2)	valence	(Pd/a_{Pd}) slope	(r^2)	valence
Oxidizing region						
1300 °C (1–3)	0.26 ± 0.01	(0.999)	1.03	0.26 ± 0.01	(0.999)	1.03
1400 °C (9–13)	0.26 ± 0.01	(0.999)	1.05	0.26 ± 0.01	(0.999)	1.05
1480 °C (19–22)	0.25 ± 0.01	(0.998)	0.99	0.25 ± 0.01	(0.999)	0.98
Reducing region						
1300 °C (3–8)	0.14 ± 0.01	(0.961)	0.55	0.14 ± 0.01	(0.960)	0.54
1400 °C (13–18)	0.15 ± 0.01	(0.977)	0.60	0.14 ± 0.01	(0.974)	0.56

Table 4. *Slope of log (Au solubility) vs. log fO_2 and effective valence of Au in silicate melts*

Conditions (Nos. of experiments)	(Au/X_{Au}) slope	(r^2)	valence	(Au/a_{Au}) slope	(r^2)	valence
Oxidizing region						
1300 °C (1–3)	0.23 ± 0.005	(1.000)	0.93	0.23 ± 0.004	(1.000)	0.93
1400 °C (9–13)	0.24 ± 0.013	(0.991)	0.95	0.24 ± 0.013	(0.992)	0.95
1480 °C (19–22)	0.22 ± 0.012	(0.994)	0.86	0.22 ± 0.012	(0.994)	0.89
Reducing region						
1300 °C (5–8)	-0.058 ± 0.006	(0.976)	−0.025	-0.054 ± 0.006	(0.974)	−0.025
1400 °C (14–18)	-0.076 ± 0.039	(0.567)	−0.306			
(16–18)				-0.46 ± 0.17	(0.88)	−1.85

however, not well defined. In the absence of a sufficient number of data points and, in addition of considerable scattering of the data (for **1400 °C the Au solubility at pure O_2 is even lower than that in air!**) the lower valence trend is very uncertain. In any case all data points in regions I + II are consistent with the assumption of Au^{1+} as Au-specie in the silicate melt (see Table 4).

A dramatic change in the behaviour of Au is seen in region III. The Au solubility begins to increase with decreasing fO_2 (Fig. 4c, d), yielding a negative formal Au valence (Table 4). Such a behavior was found by *Amosse* et al. (1990) for Pt and Ir solubilities in silicate melts. According to their explanation zero-valent Ir (and Pt) present in the melt would be passivated by the formation of Ir (and Pt) oxide layers on the surface of the metals by the reaction:

$$Ir^0(melt) + O_2 = IrO_2(Me) \quad (9)$$

This explanation can, however, be excluded for the observed increase of Au solubility with decreasing fO_2. The solubilities of Au and Pd show the opposite behavior, in spite of the fact, that both metals (in AuPd-alloys) were *simultaneously* equilibrated with the silicate melt. A more likely explanation is that additional Au is

dissolved by the formation of Au-silicides, according to the reaction:

$$\mathrm{Au(metal)} + x \cdot \mathrm{SiO_2\ (melt)} = \mathrm{AuSi_x\ (melt)} + x \cdot \mathrm{O_2} \quad (10)$$

$$\log X_{\mathrm{AuSix}}\ (\mathrm{melt}) = -x \cdot \log \mathrm{fO_2} + \log a_{\mathrm{Au}}\ (\mathrm{metal}) + \log(K_{10} \cdot a^{x}_{\mathrm{SiO_2}} / \gamma_{\mathrm{AuSi_x}}) \quad (11)$$

where K_{10} is the equilibrium constant of reaction (10).

At constant temperature and melt composition (K_{10}, $a_{\mathrm{SiO_2}}$, $\gamma_{\mathrm{AuSi_x}}$ are constant) and for the same alloy composition (a_{Au} const.) we would expect increasing Au concentration with decreasing $\mathrm{fO_2}$. It is also conceivable that excess gold is present as carbide ($\mathrm{AuC_x}$):

$$\mathrm{Au(Me)} + x \cdot \mathrm{CO\ (gas)} = \mathrm{AuC_x\ (melt)} + x/2 \cdot \mathrm{O_2} \quad (12)$$

Since there are no data, neither on Au-silicides nor on Au-carbides dissolved in silicate melts, we have no way to distinguish between these two possibilities. One way would be to use C-free gases for controlling $\mathrm{fO_2}$.

Dependence of Au- and Pd-solubilities on temperature

In addition to the determination of Au- and Pd-solubilities at various oxygen fugacities at 1300 °C, 1400 °C and 1480 °C, four additional experiments were made at fixed $\mathrm{fO_2}$ (air) to better define the dependence of solubilities on temperature for Au and Pd (see Table 2 for the data and Table 5 for regression parameters).

Results are plotted in Figs. 5a and b. For Pd solubility the temperature slope is positive, opposite to that of the temperature dependence of solubilities usually found for the iron group elements (see, for example, *Holzheid* et al., 1994, for Ni, Co and Mo), but in agreement with the data of *Borisov* et al. (1994a) on pure Pd solubility. Even the absolute value of the present slope (-3830 to -4100) is exactly the same (-3440 ± 700) as that determined for pure Pd solubility in air. For Au, however, the solubility behavior as function of temperature is completely different. Solubilities increase with increasing temperature up to 1350 °C, while at higher temperatures solubilities decrease (Fig. 5b).

Gold (metal/silicate) partition coefficients and global mantle/core equilibrium

The results of experiments for the determination of the Au-solubility in silicate melts may be used to calculate metal/silicate partition coefficients (see *Borisov* et al., 1994a for details):

$$D_{\mathrm{M/S}} = 1/[A \cdot C^{\mathrm{Au}}(\mathrm{sil}) \cdot \gamma(\mathrm{Au})] \quad (13)$$

Table 5. *Slope of log (Pd and Au solubility) vs. 1/T, K*

Conditions (Nos. of experiments)	$(\mathrm{Me}/X_{\mathrm{Me}})$ slope	(r^2)	$(\mathrm{Me}/a_{\mathrm{Me}})$ slope	(r^2)
Pd, 1300–1480 °C (1, 10, 19, 23–26)	-3830 ± 340	(0.963)	-4100 ± 420	(0.950)
Au, 1300–1350 °C (1, 23, 24)	-11880 ± 1030	(0.993)	-10890 ± 1210	(0.988)
Au, 1350–1480 °C (10, 19, 24–26)	90 ± 1000	(0.024)	2080 ± 950	(0.614)

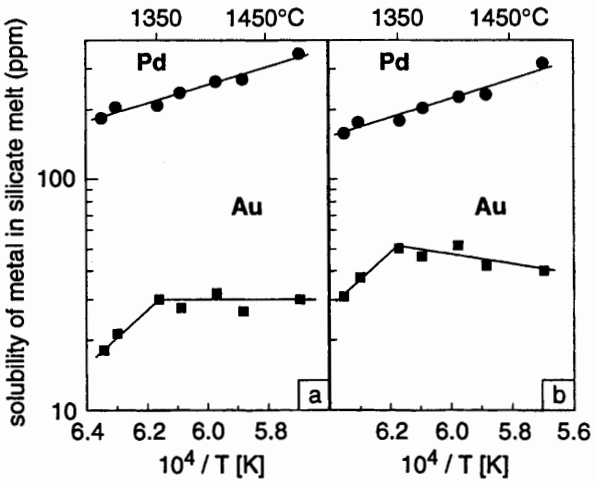

Fig. 5. Temperature dependence of Pd and Au solubilities in air: **a** assuming ideal solid solution in PdAu-alloy; **b** considering activity coefficients in PdAu-alloy. For Pd solubility the temperature slope is positive in agreement with earlier data of *Borisov* et al. (1994a) derived from experiments with pure Pd-metal. For Au, however, the slope of the temperature dependence appears to change at 1350 °C

where A is a conversion factor, C^{Au}(sil) is the solubility at the conditions required for core-mantle equilibrium, and γ(Au) is the gold activity coefficient in iron at low Au concentrations.

In order to facilitate extrapolation of Au-solubilities to higher temperatures and to lower oxygen fugacities, we calculated a single equation containing temperature and fO_2 dependence as obtained in this work. For the temperature dependence the data in air above 1350 °C (see Table 5) were used and for Au we assumed Au^{1+} as the only stable species in the silicate melt (ideal slope equal to 1/4):

$$\log (\text{Au, ppm}) = 0.25 \cdot \log fO_2 + 2080/T + 0.59 \tag{14}$$

Taking into account the temperature dependence of γ(Au) in solid iron (see section on Au-Fe thermodynamics):

$$\log(\gamma_{Au}) = 1671/T - 0.76 \tag{15}$$

the resulting equation is:

$$\log(D^{Au}) = -0.25 \cdot \log fO_2 - 3750/T + 6.7 \tag{16}$$

Thus, at 1350 °C and IW-2 we calculate $D^{Au} \sim 2.5 \cdot 10^7$ which is very close to $D^{Pd} \sim 1.6 \cdot 10^7$ for the same conditions (*Borisov* et al., 1994a). Although solubilities of Au and Pd in silicate melts are different, metal/silicate partition coefficients are similar, as the higher activity coefficient of Au in silicate melts compensates for the lower solubility. But at very high temperatures differences would increase due to the opposite behavior of Au and Pd solubilities. So for 3000 K (assuming both γ_{Au} and γ_{Pd} close to 1 in liquid iron at such high temperature) $D^{Au} \sim 2.4 \cdot 10^6$ with $D^{Au}/D^{Pd} \approx 200$.

From these and from earlier data on Ir and Pt it is clear that highly siderophile elements (HSE) show very different behavior with respect to their solubilities in silicate melts. In air Pd has the highest solubilities with 336 ppm at 1400 °C in an anorthite-diopside liquid. The corresponding solubility for Au is 51 ppm compared to about 8 ppm for Pt (*Borisov* et al., 1994b) and 2.5 ppm for Ir (*Borisov* and *Palme*, 1995a). Judging from the dependence of solubilities on oxygen fugacity of all these

metals are dissolved in silicate melt as oxides and not as metals. It appears further that the valences are generally low (around +1). The large differences in solubilities between Pd, Au on one side and Ir, Pt on the other side translate into large differences in metal-silicate partition coefficients. For example, at 1350 °C the Ir metal-silicate-partition coefficient is 10^{12}, while Au and Pd metal-silicate partition coefficients are 2.5×10^7 and 1.6×10^7 respectively (*Borisov* and *Palme*, 1995b). Although these differences become smaller at higher temperatures, as derived from extrapolations of existing data sets, they are unlikely to reach similar values which would be required if the HSE-abundances were established by a single metal-silicate equilibrium as suggested by *Murthy* (1991). It would indeed be too much of a coincidence if the temperature dependences of these partition coefficients were such that they all had a single value of about 400 at high temperatures as required by the *Murthy* (1991) model. Thus a chondritic signature of HSE, in particular a chondritic Pd/Ir-ratio, (e.g., in upper mantle rocks or in impact melts) can be taken as indicating the admixture of an unfractionated primary component.

The new and earlier data exclude the possibility that metallic PGE- and/or Au-alloys in silicate magmas or in their source region determine the abundances of PGE and Au in the melt. The presence of such alloys in the source region of MORB, at the QFM-oxygen fugacity buffer, would imply concentrations of about 5 ppm, Pd, 1 ppm Au and 10 ppb Ir in MORB (*Borisov* and *Palme*, 1995b). The actual concentrations in MORB are, however, lower by several orders of magnitude, Pd and Au are in the ppb range or lower, Ir is in the ppt range (*Hertogen* et al., 1980). It is thus unlikely that PGE- or Au-alloys play a role in producing fractionated PGE- patterns, such as high Pd/Ir-ratios, in terrestrial magmas (*Barnes* et al., 1985). The large difference in metal/silicate partition coefficients between Ir and Pd would fractionate these two elements in the residual silicates following metal segregation. However, because of the large absolute metal/silicate partition coefficients the amount of metal involved would have to be unreasonably small. Sulfides are also not good candidates since sulfide/silicate partition coefficients for Pd and Ir appear to be similar (*Peach* et al., 1994). Perhaps the prime factor in fractionating PGE from each other in terrestrial magmas is by mineral/melt partitioning (*Barnes* et al., 1985). Examples are known from olivine fractionation in komatities (*Brügmann* et al., 1987; *Zhou*, 1994).

Acknowledgments

Samples were activated in the TRIGA-reactor of the Institut für Anorganische Chemie und Kernchemie der Universität Mainz. We thank the staff of the reactor for their assistance. The help of *B. Spettel* during INAA procedures was essential. *J. Huth* is thanked for his help with the SEM. The suggestions of an anonymous reviewer were very helpful in revising the paper and are greatly appreciated. *A. Holzheid* is thanked for carefully reading the manuscript. This study was supported by the Deutsche Forschungsgemeinschaft (DFG) and in part by the Russian fund for fundamental research (93-05-9856).

References

Amosse J, Allibert M, Fischer W, Piboule M (1990) Experimental study of the solubility of platinum and iridium in basic silicate melts – implications for the differentiation of platinum-group elements during magmatic processes. Chem Geol 81: 45–53

Barnes SJ, Naldrett AJ, Gorton MP (1985) The origin of the fractionation of platinum-group elements in terrestrial magmas. Chem Geol 53: 303–323

Brügmann GE, Arndt NT, Hofmann AW, Tobschall HJ (1987) Noble metal abundances in komatitite suites from Alexo, Ontario, and Gorgona Island, Colombia. Geochim Cosmochim Acta 51: 2159–2169

Borisov A, Palme H (1995a) The solubility of Iridium in silicate melts: new data from experiments with $Ir_{90}Pd_{90}$ alloys. Geochim Cosmochim Acta 59: 481–486

Borisov A, Palme H (1995b) Metal/silicate/sulfide partition coefficients of highly siderophile elements (HSE) as derived from recent solubility data. Lunar Planet Sci XXVI: 147–148

Borisov A, Palme H, Spettel B (1994a) Solubility of Pd in silicate melts: implications for core formation in the Earth. Geochim Cosmochim Acta 58: 705–716

Borisov A, Palme H, Spettel B (1994b) The solubility of platinum in silicate melts: experiments under oxidizing conditions. Lunar Planet Sci XXV: 141–142

Capobianco CJ (1990) A method for the extraction of thermodynamic properties of alloys which are sparingly soluble in silicate melts at high temperature. Lunar Planet Sci XXI: 164–165

Gmelin Handbook of Inorganic and Organometallic Chemistry (1992) Au. Gold. Supplement B, part 1. [*Keim R, Schnager B* (eds)] Springer, Berlin Heidelberg New York Tokyo

Hamilton DL, Henderson CMB (1968) The preparation of silicate compositions by a gelling method. Mineral Mag 36: 832–838

Hertogen J, Janssens M-J, Palme H (1980) Trace elements in ocean ridge basalt glasses: implications for fractionations during mantle evolution and petrogenesis. Geochim Cosmochim Acta 44: 2125–2143

Holzheid A, Borisov A, Palme H (1995) The effect of oxygen fugacity and temperature on the solubility of nickel, cobalt, and molybdenum in silicate melts. Geochim Cosmochim Acta 58: 1975–1981

Hultgren R, Desai PD, Hawkins PD, Gleiser M, Kelly K (1973) Selected value of the thermodynamic properties of binary alloys. Am Soc Metals, New York

Jagoutz E, Palme H, Baddenhausen H, Blum K, Cendales M, Dreibus G, Spettel B, Lorenz V, Wänke H (1979) The abundances of major, minor and trace elements in the earth's mantle as derived from ultramafic nodules. Proc Lunar Planet Sci Conf 10th: 2031–2050

Jones JH, Drake MJ (1986) Geochemical constraints on core formation in the Earth. Nature 322: 221–228

Kimura K, Lewis RS, Anders E (1974) Distribution of gold and rhenium between nickel-iron and silicate melts: implications for the abundances of siderophile elements of the Earth and Moon. Geochim Cosmochim Acta 38: 683–701

Kubaschewski O, Counsell JF (1971) Thermodynamische Eigenschaften des Systems Gold-Platin-Palladium. Mo Chem 102: 1724–1728

Murthy VR (1991) Early differentiation of the Earth and the problem of mantle siderophile elements: a new approach. Science 253: 303–306

Okamoto H, Massalsky TB (1985) The Au-Pd (gold-palladium) system. Bull Alloy Phase Diagrams 6: 229–234

Peach CL, Mathez EA, Keays RR, Reeves SJ (1994) Experimentally determined sulfide melt-silicate melt partition coefficients for iridium and palladium. Chem Geol 117: 361–377

Rammensee W (1978) Verteilungsgleichgewichte von Spurenelementen zwischen Metallen und Silikaten. Thesis, Universität Mainz

Thompson JB Jr (1967) Thermodynamic properties of simple solutions In: *Abelson PH* (ed) Researches in geochemistry, vol 2. Wiley & Sons, pp 340–361

Weyl WA (1951) Colored glasses. The Society of Glass Technology, Sheffield
Zhou M-F (1994) PGE distribution in 2.7-Ga layered komatiite flows from the Belingwe greenstone belt, Zimbabwe. Chem Geol 118: 155–172

Authors' addresses: Dr. *A. Borisov*, Dr. *H. Palme*, Mineralogisch-Petrographisches Institut, Universität zu Köln, Zülpicher Strasse 49b, D-50674 Köln, Federal Republic of Germany

Verleger: Springer-Verlag KG, Sachsenplatz 4–6, A-1201 Wien. – Herausgeber: Prof. Dr. E. F. Stumpfl, Institut für Geowissenschaften der Montanuniversität, Franz-Josef-Straße 18, A-8700 Leoben. – Redaktion: Franz-Josef-Straße 18, A-8700 Leoben. – Satz und Umbruch: Thomson Press (India) Ltd., New Delhi; Offsetdruck: Novographic, Ing. W. Schmid, Maurer-Lange-Gasse 64, A-1238 Wien. – Verlagsort: Wien – Herstellungsort: Wien. – Printed in Austria.